Chapter 1

Dimensional Crossover of the Dephasing Time in Disordered Mesoscopic Rings: From Diffusive through Ergodic to 0D Behavior

M. Treiber, O.M. Yevtushenko, F. Marquardt and J. von Delft

Arnold Sommerfeld Center and Center for Nano-Science, Ludwig Maximilians University, Munich, D-80333, Germany

I.V. Lerner

School of Physics and Astronomy, University of Birmingham, Birmingham, B15 2TT, UK

We analyze dephasing by electron interactions in a small disordered quasi-one dimensional ($1D$) ring weakly coupled to leads, where we recently predicted a crossover for the dephasing time $\tau_\varphi(T)$ from diffusive or ergodic $1D$ ($\tau_\varphi^{-1} \propto T^{2/3}, T^1$) to $0D$ behavior ($\tau_\varphi^{-1} \propto T^2$) as T drops below the Thouless energy $E_{\rm Th}$.[1] We provide a detailed derivation of our results, based on an influence functional for quantum Nyquist noise, and calculate all leading and subleading terms of the dephasing time in the three regimes. Explicitly taking into account the Pauli blocking of the Fermi sea in the metal allows us to describe the $0D$ regime on equal footing as the others. The crossover to $0D$, predicted by Sivan, Imry and Aronov for $3D$ systems,[2] has so far eluded experimental observation. We will show that for $T \ll E_{\rm Th}$, $0D$ dephasing governs not only the T-dependence for the smooth part of the magnetoconductivity but also for the amplitude of the Altshuler-Aronov-Spivak oscillations, which result only from electron paths winding around the ring. This observation can be exploited to filter out and eliminate contributions to dephasing from trajectories which do not wind around the ring, which may tend to mask the T^2 behavior. Thus, the ring geometry holds promise of finally observing the crossover to $0D$ experimentally.

1.1. Introduction

Over the last twenty-five years many theoretical and experimental works addressed quantum phenomena in mesoscopic disordered metallic rings.[3]

This subject was launched in part by several seminal papers by Joe Imry and his collaborators [4–11], and continues to be of great current interest. One intensively-studied topic involves persistent currents, which can flow without dissipation due to quantum interference in rings prepared from normal metals.[4,12–15] Attention was also paid to Aharonov-Bohm oscillations in the conductance through a mesoscopic ring attached to two leads,[5–7,10,16]and the closely related oscillations of the negativeweak localization (WL) correction to the magnetoconductivity.[17,18]These oscillations result from the interference of closed trajectories which have a non-zero winding number acquiring the Aharonov-Bohm phase. Both persistent currents and magnetooscillations require the ring to be phase coherent, since any uncertainty of the quantum phase due to the environment or interactions immediately suppresses all interference phenomena.[19]

The mechanism of dephasing in electronic transport and its dependence on temperature T in disordered conductors was studied in numerous theoretical[2,19–27] and experimental[28–35] works. The characteristic time scale of dephasing is called the dephasing time τ_φ. At low temperatures phonons are frozen out and dephasing is mainly due to electron interactions, with the dephasing time $\tau_\varphi(T)$ increasing as T^{-a} when $T \to 0\,,\ a > 0$.

The scaling of the dephasing time with temperature depends on the dimensionality of the sample.[20] It was predicted in a pioneering paper by Sivan, Imry and Aronov[2] that the dephasing time in a disordered quantum dot shows a dimensional crossover from $\tau_\varphi \propto T^{-1}$, typical for a $2D$ electron gas,[20] to $\tau_\varphi \propto T^{-2}$ when the temperature is lowered into the $0D$ regime:

$$\hbar/\tau_\varphi \ll T \ll \hbar/\tau_{\rm Th}\,, \tag{1.1}$$

where $\tau_{\rm Th} = \hbar/E_{\rm Th}$ is the Thouless time, i.e. the time required for an electron to cross (diffusively or ballistically) the mesoscopic sample; $E_{\rm Th}$ is the Thouless energy. In this low-T, 0D regime, the coherence length and the thermal length are both larger than the system size, independent of geometry and real dimensionality of the sample. In this regime WL is practically the only tool to measure the T-dependence of dephasing in mesoscopic wires or quantum dots (the mesoscopic conductance fluctuations go over to a universal value of order e^2/h for $T \ll {E_{\rm Th}}^3$).

Although the $\tau_\varphi \propto T^{-2}$ behavior is quite generic, arising from the fermionic statistics of conduction electrons, experimental efforts[31–33] to observe it have so far been unsuccessful. The reasons for this are today still unclear. Conceivably dephasing mechanisms other than electron interactions were dominant, or the regime of validity of the $0D$ description

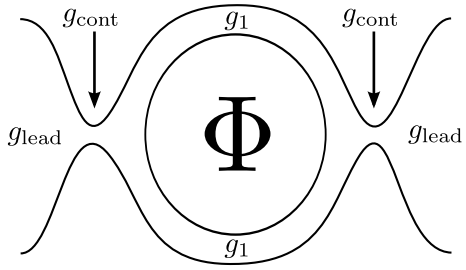

Fig. 1.1. A ring weakly coupled to leads: We assume a metallic system, where the conductance at the contacts $g_{\rm cont}$ is much smaller than the conductance of the ring g_1 and of the lead $g_{\rm lead}$, i.e. $(g_{\rm lead}, g_1) \gg g_{\rm cont} \gg 1$. This assures (a) that the average time electrons spend in the ring ($\tau_{\rm dw}$) is much larger than the average time they need to explore the whole ring ($\tau_{\rm Th}$) and (b) that the probability for electrons which escaped from the ring to return back to it is small.

had not been reached. In any case, other ways of testing the dimensional crossover for τ_φ are desirable.

In a recent paper,[1] we described the crossover of the dephasing time to the $0D$ regime in a mesoscopic ring weakly coupled to leads. We considered a ring of the type shown in Fig. 1.1 with dimensionless $1D$ conductance

$$g_1 = \frac{h\sigma_0}{e^2}\frac{A}{L}\,, \tag{1.2}$$

where A and L are the ring's cross section and circumference and σ_0 is its classical Drude conductivity. In the present paper we give a detailed derivation of our results based on an influence functional approach for *quantum noise*. This approach explicitly takes into account the Pauli blocking of the electrons in the metal, which will allow us to describe quantitatively all regimes of the dephasing time in a quasi-$1D$ ring on an equal footing and to calculate first order correction terms to the dephasing time. In particular, we will see that Pauli blocking dominates the regime of $0D$ dephasing. We find that in the $0D$ regime, T^{-2} behavior also emerges for the amplitude of the Altshuler-Aronov-Spivak (AAS) oscillations of the conductivity[17] in a magnetic field, which arise from pairs of time-reversed paths encircling the ring at least once. A necessary requirement to reach this regime is that electron trajectories are effectively confined in the system. Thus the conductance through the contact, $g_{\rm cont}$, is assumed to be much smaller than g_1, such that the time an electron spends inside the ring, the dwelling time $\tau_{\rm dw}$, is much larger than the time an electron needs to explore the whole ring, i.e. the Thouless time $\tau_{\rm Th}$.

We will show below that after subtracting from the amplitude of the AAS-oscillations the non-oscillating background, only contributions to dephasing from paths encircling the ring will contribute. However, some of these paths may involve loops which not only encircle the ring, but along the way also enter the lead and reenter the ring (see Fig. 1.6(b) below). Such lead-ring cross-contributions to dephasing will contribute a non-$0D$ T-dependence to the conductance and hence tend to mask the $0D$ behavior. We shall argue that by additionally choosing the conductance of the connected leads, $g_{\rm lead}$, to be larger than $g_{\rm cont}$, dephasing due to lead-ring cross-contributions, can be neglected, and the remaining contributions will be characterized by $0D$ dephasing.

1.2. Dephasing and weak localization

In a disordered metal, the conductivity is reduced by coherent backscattering of the electrons from impurities, an effect known as weak localization (WL). In a semi-classical picture it can be understood as the constructive interference of closed, time-reversed random-walks through the metal's impurity landscape. It is most pronounced in systems of low dimensionality d where the integrated return probability becomes large for long times. For an infinite system characterized by the diffusion constant $D = v_F l/d$ (v_F is the Fermi velocity and l is the mean free path), the probability of a random walk of duration t to return back to its origin is given by

$$\mathcal{C}_0(t) = (4\pi D t)^{-d/2}\,. \tag{1.3}$$

To leading order in $1/g_1$, the relative correction to the conductance (1.2) can be written as

$$\Delta g = \frac{\Delta\sigma}{\sigma_0} = -\frac{1}{\pi\nu}\int_0^\infty \mathrm{d}t\,\mathcal{C}(t)\,, \tag{1.4}$$

where ν is the density of states per volume in the ring and we have set $\hbar = 1$ henceforth. The function $\mathcal{C}(t)$ is the so called Cooperon propagator corresponding to the interference amplitude of the time-reversed random walks. $\mathcal{C}(t)$ reduces to Eq. (1.3) if time-reversal symmetry is fully preserved. Processes which destroy this symmetry lead to a suppression of this contribution at long times, since the random walks and their time-reversed counterparts acquire a different phase. The model we are considering assumes a suppression of the Cooperon of the following form

$$\mathcal{C}(t) \equiv \mathcal{C}_0(t)\exp\left[-t/\tau_H - t/\tau_{\rm dw} - \mathcal{F}(t)\right]\,. \tag{1.5}$$

In Eq. (1.5), we consider dephasing due to the effect of an external magnetic field leading to the cutoff $\tau_H \sim 1/H$ of the integral in Eq. (1.4).[43] Furthermore, our model of an almost isolated ring assumes an average dwelling time, $\tau_{\rm dw}$, of the electrons in the ring.[45]

Our primary interest is the effect of electron interactions, which we describe in terms of the *Cooperon decay function* $\mathcal{F}(t)$, which grows with time and may be used to define a dephasing time via

$$\mathcal{F}(\tau_\varphi) = 1\,. \tag{1.6}$$

Dephasing due to electron interactions can be understood roughly as follows: At finite temperatures the interactions lead to thermal fluctuations (noise) of the electron's potential energy $V(\mathbf{x},t)$. Then the closed paths contributing to WL and their time-reversed counterparts effectively "see" a different local potential, leading to a phase difference. This is most clearly seen in a path integral representation of the Cooperon in a time-dependent potential,[20] which is given by

$$\mathcal{C}(t) \propto \int_{\mathbf{x}(0)=\mathbf{x}_0}^{\mathbf{x}(t)=\mathbf{x}_0} \mathcal{D}\mathbf{x}\; e^{i\varphi(t)} e^{-\int_0^t {\rm d}t_1\, \mathcal{L}(t_1)}\,. \tag{1.7}$$

Here the Lagrangian $\mathcal{L}(t_1) = \dot{\mathbf{x}}^2(t_1)/4D$ describes diffusive propagation, and $\varphi(t)$ is a phase corresponding to the time-reversed structure of the Cooperon:

$$\varphi(t) = \int_0^t {\rm d}t_1\; [V(\mathbf{x}(t_1),t_1) - V(\mathbf{x}(t_1),t-t_1)]\;. \tag{1.8}$$

Assuming that the noise induced by electron interactions is Gaussian, the decay function $\mathcal{F}(t)$ in Eq. (1.5) can be estimated from $\mathcal{F}(t) = \frac{1}{2}\langle\overline{\varphi^2}\rangle_{\rm crw}$, where $\overline{\cdots}$ denotes averaging over realizations of the noise and $\langle\ldots\rangle_{\rm crw}$ over closed random walks of duration t from $\mathbf{x}_0$ back to $\mathbf{x}_0$. $\mathcal{F}(t)$ is then given in terms of a difference of the noise correlation functions, taken at reversed instances of time:

$$\mathcal{F}(t) = \int_0^t {\rm d}^2 t_{1,2} \left\langle \overline{VV}(\mathbf{x}_{12},t_{12}) - \overline{VV}(\mathbf{x}_{12},\bar{t}_{12}) \right\rangle_{\rm crw}\,. \tag{1.9}$$

Here $t_{12} = t_1 - t_2$ and $\bar{t}_{12} = t_1 + t_2 - t$, while $\mathbf{x}_{12} = \mathbf{x}(t_1) - \mathbf{x}(t_2)$ is the distance of two points of the closed random walk taken at times t_1 and t_2. For an infinite wire and the case of classical Nyquist noise (defined in Eq. (1.11) below), Eq. (1.9) has been shown[26,27] to give results practically equivalent to the exact results obtained in Ref. [20].

1.3. Thermal noise due to electron interactions

Electron interactions in the metal lead to thermal fluctuations of the electric field **E**, producing so-called Nyquist noise. In the high temperature limit, it can be obtained from the classical Fluctuation-Dissipation Theorem leading to a field-field correlation function in 3D of the form

$$\overline{\mathbf{E}\mathbf{E}}(\mathbf{q},\omega) \xrightarrow{|\omega|\ll T} \frac{2T}{\sigma_0}\,. \tag{1.10}$$

Note that the fluctuations of the fields do not depend on $\mathbf{q}$ or ω, i.e. they correspond to white noise in space and time. To describe dephasing in a quasi-1D wire, we need the correlation function of the corresponding scalar potentials V in a quasi-1D wire. Since $E = \frac{1}{e}\nabla V$, the noise correlator that corresponds to the classical limit (1.10) has the form

$$\overline{VV}_{\rm class}(\mathbf{q},\omega) = \frac{2Te^2}{\sigma_0}\frac{1}{\mathbf{q}^2}\,. \tag{1.11}$$

This so-called classical Nyquist noise is frequency independent, i.e. corresponds to "white noise". For present purposes, however, we need its generalization to the case of quantum noise, valid for arbitrary ratios of $|\omega|/T$. In particular, $\overline{VV}$ is expected to become frequency-dependent: it should go to zero for $|\omega| \gg T$, since the Pauli principle prevents scattering processes into final states occupied by other electrons in the Fermi sea.[38] A careful analysis of quantum noise has been given recently in Ref. [26] and Ref. [27]. The authors derived an effective correlation function for the quantum noise potentials that properly accounts for the Pauli principle. It is given by

$$\overline{VV}(\mathbf{q},\omega) = {\rm Im}\mathcal{L}^R(\mathbf{q},\omega)\,\frac{\omega/2T}{\sinh\left(\omega/2T\right)^2} \tag{1.12}$$

with

$$\mathcal{L}^R(\mathbf{q},\omega) = -\frac{D\mathbf{q}^2 - i\omega}{2\nu D\mathbf{q}^2 + (D\mathbf{q}^2 - i\omega)/V(\mathbf{q})}\,; \tag{1.13}$$

$V(q)$ is the Fourier-transformed bare Coulomb potential (not renormalized due to diffusion) in the given effective dimensionality.

If the momentum and energy transfer which dominates dephasing is small then the second term of the denominator of Eq. (1.13) can be neglected so that Eq. (1.13) reduces to

$${\rm Im}\mathcal{L}^R(\mathbf{q},\omega) \simeq \frac{\omega}{2\nu D\mathbf{q}^2}\,. \tag{1.14}$$

This simplification holds true, in particular, in the high temperature (diffusive) regime where $\omega \ll T$.[20] We will argue below (see Eqs. (1.54) to (1.57)) that the same simplification can be used in the low temperature regime where $|\omega| \sim T \lesssim E_{\rm Th}$.[1]

Inserting Eq. (1.14) in Eq. (1.12) with $\sigma_0 = 2e^2\nu D/A$, where A is the cross-section perpendicular to the current direction, we obtain

$$\overline{VV}(\mathbf{q},\omega) = \frac{2e^2\,T}{\sigma_0 A}\,\frac{1}{\mathbf{q}^2}\,\left(\frac{\omega/2T}{\sinh(\omega/2T)}\right)^2 . \tag{1.15}$$

In the time and space domain, this correlator factorizes into a product of time- and space-dependent parts:

$$\overline{VV}(\mathbf{x},t) = \frac{2e^2\,T}{\sigma_0 A}\,Q(\mathbf{x})\,\delta_T(t)\,, \tag{1.16}$$

where $\delta_T(t)$ is a broadened delta function of width $1/T$ and height T:

$$\delta_T(t) = \pi T w(\pi\,T\,t)\,, \qquad w(y) = \frac{y\coth(y)-1}{\sinh^2(y)}\,. \tag{1.17}$$

The fact that the noise correlator (1.16) is proportional to a *broadened* peak $\delta_T(t)$ is a direct consequence of the effects of Pauli blocking. Previous approaches often used a sharp Dirac-delta peak instead. In the frequency domain this corresponds to white noise and leads to (1.11), instead of our frequency-dependent form (1.12). Such a "classical" treatment reproduces correct results for the dephasing time when processes with small energy transfers $|\omega| \ll T$ dominate. However, it has been shown in Ref. [2] that this is in fact not the case in the $0D$ limit $T \ll E_{\rm Th}$, where the main contribution to dephasing is due to processes with $|\omega| \simeq T$. Thus, the results become dependent on the form of the cutoff that eliminates modes with $|\omega| > T$ to account for the Pauli principle. For such purposes, previous treatments typically introduced a sharp cutoff, $\theta(T-|\omega|)$, by hand. However, the precise form of the cutoff becomes important in an analysis interested not only in qualitative features, but quantitative details. The virtue of (1.11) is that it encodes the cutoff in a quantitatively reliable fashion. (For example, it was shown[26] to reproduce a result first obtained in Ref. [23], namely the subleading term in an expansion of the large-field magnetoconductance (for quasi-1D wires) in powers of the small parameter $1/\sqrt{T\tau_H}$.)

The position-dependent part of Eq. (1.16), the so-called diffuson at zero frequency $Q(\mathbf{x})$, is the time-integrated solution of the diffusion equation. In the isolated system, it satisfies

$$-\Delta Q(\mathbf{x}) = \delta(\mathbf{x})\,, \tag{1.18}$$

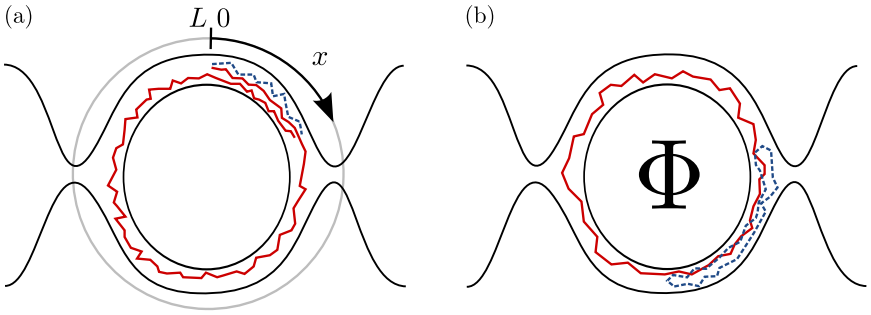

Fig. 1.2. (a) Illustration of our choice of the coordinate system: Both paths have the same start and end point ($0 \mapsto x$), but the dashed path has winding number $n = 0$ and the solid path $n = 1$. (b) Two *closed* paths in the ring contributing to the Cooperon. The contribution of the solid path (with winding number $n = 1$) is affected by the flux Φ, since the path (and it's time-reversed counterpart) acquire an Aharonov-Bohm phase when interfering with itself at their origin. This gives rise to the Altshuler-Aharonov-Spivak oscillations. The dashed path with $n = 0$ is unaffected by the flux, since the acquired phase at the origin is zero.

with given boundary conditions, which govern the distribution of the eigenmodes of Q. In an isolated system, where a $\mathbf{q} = 0$ mode is present, $Q(\mathbf{x})$ diverges. However, the decay function is still regular, since terms in Q which do not depend on $\mathbf{x}$ simply cancel out in Eq. (1.9) and cannot contribute to dephasing.

To evaluate the decay function Eq. (1.9), we note that only the factor $Q(\mathbf{x})$ in Eq. (1.16) depends on $\mathbf{x}$, thus, the average $\langle Q(\mathbf{x})\rangle_{\mathrm{crw}}$ has to be calculated. This will be done in the next section for an almost isolated ring. Then, after a qualitative discussion in 1.5, we proceed by evaluating $\mathcal{F}(t)$ in section 1.6.

1.4. Diffusion in the almost isolated ring

The probability density of a random walk in a $1D$, infinite, isotropic medium to travel the distance x in time t is given by

$$P_0(x,t) = \frac{1}{\sqrt{4\pi D t}}\, e^{-x^2/4Dt}\,. \tag{1.19}$$

In an isolated ring, electrons can reach each point without or after winding around the ring n times, where n is called *winding number*. Denoting the probability density for the latter type of path by $P_n(x,t)$, the diffusion

probability density can be expanded in n as

$$P(x,t) = \sum_{n=-\infty}^{+\infty} P_n(x,t)\,, \quad P_n(x,t) = \frac{1}{\sqrt{4\pi D t}}\, e^{-(x+nL)^2/4Dt}\,, \qquad (1.20)$$

where L is the circumference of the ring and $x \in [0, L]$ is the cyclic coordinate along the ring, see Fig. 1.2(a). To model the effect of the two contacts of the ring, we assume that an electron, on average, stays inside the ring only for the duration of the dwelling time $\tau_{\rm dw}$, introduced in Eq. (1.5), and then escapes with a vanishing return probability. This simplified model of homogeneous dissipation, strictly applicable only in the limit $\tau_{\rm Th} \ll \tau_{\rm dw}$ and for a very large lead conductance, captures all the essential physics of the $0D$ crossover we are interested in. Our present assumptions lead to the following replacement of the diffusion probability density:

$$P(x,t) \to P(x,t)\; e^{-t/\tau_{\rm dw}}\,. \qquad (1.21)$$

Furthermore, the spatial dependence of the noise correlation function (1.13) acquires an additional dissipation term in the denominator. Thus, in contrast to the isolated case, $Q(x)$ now satisfies the Laplace transform of the diffusion equation, given by

$$\left[\frac{1}{L_{\rm dw}^2} - \Delta\right] Q(x) = \delta(x)\,, \qquad (1.22)$$

where $L_{\rm dw} = \sqrt{\tau_{\rm dw} D}$. For a ring with circumference L we obtain

$$Q(x) = \frac{L_{\rm dw}}{2}\, \frac{\cosh\Big([L - 2|x|]/2L_{\rm dw}\Big)}{\sinh(L/2L_{\rm dw})}\,. \qquad (1.23)$$

We can expand Eq. (1.23) for the almost isolated ring in powers of $\tau_{\rm Th}/\tau_{\rm dw} \ll 1$:

$$Q(x) \approx C - \frac{|x|}{2}\left(1 - \frac{|x|}{L}\right) + \mathcal{O}\left(\frac{\tau_{\rm Th}}{\tau_{\rm dw}}\right)\,, \qquad (1.24)$$

where the x-independent first term, $C = L\tau_{\rm dw}/\tau_{\rm Th}$, describes the contribution of the zero mode. As expected, see the discussion after Eq. (1.18), it diverges in the limit $\tau_{\rm Th}/\tau_{\rm dw} \to 0$.

Having described the diffuson in our model of the almost isolated ring, we can proceed by calculating the closed random walk average (crw) of Eq. (1.24). We will see below that we need to consider the random walk

average with respect to closed paths with a specific winding number n only. For an isolated ring, using Eq. (1.20), it can be written as

$$\langle Q\rangle_{\rm crw}(t_{12},n)=\int_0^L {\rm d}^2x_{1,2}\,Q(x_{12})P_{\rm crw}(x_{12},t_{12},n)\,, \tag{1.25}$$

with

$$P_{\rm crw}(x_{12},t_{12},n)=\sum_{i+j+k=n}\frac{P_i(x_{01},t_1)P_j(x_{12},t_{21})P_k(x_{20},t-t_2)}{P_n(0,t)}\,, \tag{1.26}$$

where we used the notation $x_{\alpha\beta}=x_\alpha-x_\beta$ and $t_{\alpha\beta}=t_\alpha-t_\beta$. Obviously, the replacement (1.21) does not affect this averaging procedure, so that it remains valid in our model of homogeneous dissipation. Note that the expression (1.26) depends in fact only on x_{12} and not on x_0, as can be verified by integrating both sides of the equation over x_0 using the following semi-group property in the ring:

$$\int_0^L {\rm d}x_2\,P_l(x_{12},t_1)P_m(x_{23},t_2)=P_{l+m}(x_{13},t_1+t_2)\,. \tag{1.27}$$

Doing the average of Eq. (1.23) according to Eq. (1.25), we finally obtain

$$\langle Q\rangle_{\rm crw}(t_{12},n)=C-\frac{L}{2}\sum_{k=1}^{\infty}\frac{\cos(2\pi knu)}{(\pi k)^2}e^{-(2\pi k)^2\,E_{\rm Th}\,t_{12}(1-t_{12}/t)}\,. \tag{1.28}$$

It follows that a finite dissipation rate does not affect the decay function to leading order in $\tau_{\rm Th}/\tau_{\rm dw}$.

For the Cooperon, an expansion similar to Eq. (1.20) can be done. In addition to that, the dependence of the Cooperon on an external magnetic field changes due to the ring geometry. It not only leads to the suppression of the Cooperon at long times, but also, due to the Aharonov-Bohm effect, to Altshuler-Aronov-Spivak oscillations[17] of the WL-correction, see Fig. 1.2(b). Combining these remarks with Eq. (1.5) and inserting Eq. (1.3) with $d=1$, we write the Cooperon in our model as

$$\mathcal{C}(t)=\sum_{n=-\infty}^{+\infty}\frac{e^{-(nL)^2/4Dt}}{\sqrt{4\pi Dt}}e^{-t/\tau_H-t/\tau_{\rm dw}-\mathcal{F}_n(t)}e^{in\theta}\,, \tag{1.29}$$

where $\theta=4\pi\phi/\phi_0$ and $\phi=\pi(L/2\pi)^2H$ is the flux through the ring ($\phi_0=2\pi c/e$ is the flux quantum). Note that the decay function $\mathcal{F}$ is now a function of n: Since we used an expansion in winding numbers n, we should consider the phase (1.8) acquired by paths with the winding number n only. Thus, the crw-average in Eq. (1.9) has to be performed with respect to paths with given winding number n only, as anticipated in Eq. (1.25).

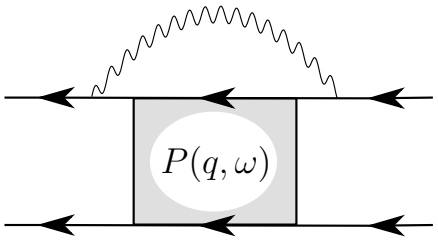

Fig. 1.3. Typical diagram from the expansion of the Cooperon self energy. The shaded area denotes impurity lines, described by the diffusion propagator Eq. (1.31). The upper solid lines correspond to a retarded electron Green's function and the lower to an advanced (or vice versa). Wiggly lines denote electron interactions, described by Eq. (1.16).

1.5. Qualitative picture from the perturbative expansion of the Cooperon

In our previous paper[1] we showed how all the regimes of the dephasing time in an isolated ring can be understood qualitatively from the influence functional picture. In particular, we demonstrated how $0D$ dephasing emerges from the assumption of a noise field that is effectively "frozen" on the time scale $\tau_{\rm Th}$ (since $|\omega| \simeq T \ll E_{\rm Th}$), leading to a drastically reduced dephasing rate. The qualitative behavior of τ_φ also follows from the standard perturbative expression for the Cooperon self-energy. Such self-energy diagrams are of the type shown in Fig. 1.3 and were first evaluated in Ref. [21]. This diagram and its complex conjugate give contributions to the dephasing time of the form

$$\frac{1}{\tau_\varphi} \propto \int \mathrm{d}\omega \int \mathrm{d}q\, \overline{VV}(q,\omega)\, \mathrm{Re}[P(q,\omega)]\ , \tag{1.30}$$

where the diffuson $P(q,\omega)$ is given by the Fourier transform of Eq. (1.19):

$$P(q,\omega) = \frac{1}{Dq^2 - i\omega}\,. \tag{1.31}$$

We have already mentioned that large energy transfers are suppressed according to Eq. (1.15) leading to an upper cutoff at T of the frequency integration. Furthermore, it was shown in Refs. [26,27] that vertex contributions to these self-energy diagrams cure the infrared divergences in the frequency integration, leading to a cutoff at $1/\tau_\varphi$. Such fluctuations are simply too slow to influence the relevant paths. Note that in contrast to the perturbative treatment presented in this section, the path integral calculation leading to the expression Eq. (1.9) for the decay function is free of

these IR divergences. In fact, it was shown that the first term of Eq. (1.9) corresponds, when compared to a diagrammatic evaluation of the Cooperon self-energy, to the so-called self-energy contributions (shown in Fig. 1.3), while the second term corresponds to the so-called vertex contributions.

In the ring geometry, the diffuson has quantized momenta and the $q = 0$ mode can not contribute. For a qualitative discussion we may take this into account by inserting a lower cutoff $1/L$ of the momentum integration.

Taking into account the above remarks, we can estimate the dephasing time as

$$\frac{1}{\tau_\varphi} \propto \frac{T}{g_1 L} \int_{1/\tau_\varphi}^{T} \mathrm{d}\omega \int_{1/L}^{\infty} \mathrm{d}q \, \frac{D}{(Dq^2)^2 + \omega^2} \,. \tag{1.32}$$

Eq. (1.32) illustrates succinctly that the modes dominating dephasing lie near the infrared cutoff ($\omega \simeq \tau_\varphi^{-1}$ or E_{Th}) for the diffusive or ergodic regimes, but near the ultraviolet cutoff $\omega \simeq T$ for the $0D$ regime, which is why, in the latter, the broadening of $\delta_T(t)$ becomes important. Performing the integrals in Eq. (1.28) and solving for τ_φ selfconsistently, we find three regimes:

(1) The *diffusive regime*, for $\tau_T \ll \tau_\varphi \ll \tau_{\mathrm{Th}}$, with

$$\tau_\varphi \propto (g_1/\sqrt{E_{\mathrm{Th}} T})^{2/3} \,; \tag{1.33}$$

(2) the *ergodic regime*, for $\tau_T \ll \tau_{\mathrm{Th}} \ll \tau_\varphi$, with

$$\tau_\varphi \propto g_1/T \,; \tag{1.34}$$

(3) and the $0D$ *regime*, reached at $\tau_{\mathrm{Th}} \ll \tau_T \ll \tau_\varphi$, with

$$\tau_\varphi \propto g_1 E_{\mathrm{Th}}/T^2 \,. \tag{1.35}$$

Here, $\tau_T = \sqrt{D/T}$ is the thermal time. Expressing (1.35) in terms of the level spacing $\delta = E_{\mathrm{Th}}/g_1$ we find $\tau_\varphi \delta \propto E_{\mathrm{Th}}^2/T^2$. This ratio is $\gg 1$ in the 0D regime, implying that dephasing is so weak that the dephasing rate $1/\tau_\varphi$ is smaller than the level spacing.

1.6. Results for the Cooperon decay function

For a systematic analysis of the Cooperon decay function, we rewrite Eq. (1.9) in terms of an integral over the dimensionless variable $u = t_{12}/t$:

$$\mathcal{F}_n(t) = \frac{4\pi T t}{g_1} \int_0^1 \mathrm{d}u \, z(u) \, q_n(u) \,, \tag{1.36}$$

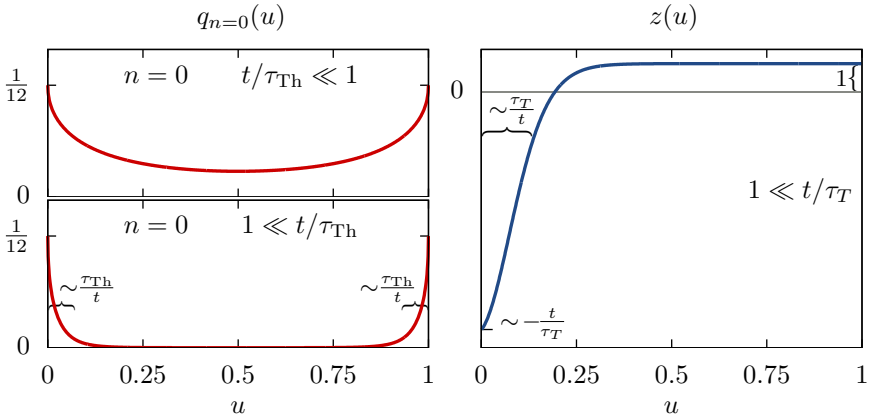

Fig. 1.4. Functions $q_{n=0}(u)$ (left panel) defined in Eq. (1.38) and $z(u)$ (right panel) defined in Eq. (1.37).

where the kernel

$$z(u) = -2\pi Tt\,(1-u)\,w(\pi Ttu) + \int_{-\pi Ttu}^{\pi Ttu} \mathrm{d}v\, w(v) \tag{1.37}$$

depends on the parameter $tT = t/\tau_T$, and the dimensionless crw-averaged diffuson

$$q_n(u) = \frac{\langle Q\rangle_{\rm crw}(ut) - C}{L} = -\frac{1}{2}\sum_{k=1}^{\infty} \frac{\cos(2\pi knu)}{(\pi k)^2} e^{-(2\pi k)^2\,(t/\tau_{\rm Th})\,u(1-u)}\,, \tag{1.38}$$

depends on $t/\tau_{\rm Th}$, see Eq. (1.28). Note that we can add or subtract an arbitrary number from $q_n(u)$ without changing the result, since constant terms in $q_n(u)$, describing the zero mode, do not contribute to dephasing, because of the following property of $z(u)$:

$$\int_0^1 \mathrm{d}u\, z(u) = 0\,. \tag{1.39}$$

Both functions, Eq. (1.37) and Eq. (1.38), are illustrated in Fig 1.4 in all relevant limiting cases. Note that in the regime of WL we always have $\tau_T \ll t$. In the opposite regime the interaction correction to the conductivity (Altshuler-Aronov correction) originating from the Friedel oscillations dominate,[48] which we do not consider here.

We proceed with an asymptotic evaluation of Eq. (1.36). For large $t/\tau_{\rm Th}$, $q_n(u)$ is non-zero ($\simeq \frac{1}{12}$) only in the intervals $0 < u < \tau_{\rm Th}/t$ and

$1-\tau_{\rm Th}/t<u<1$, see Fig. 1.4. For small $t/\tau_{\rm Th}$ and $n=0$ we can use the expansion

$$q_{n=0}(u)\approx\frac{1}{12}-\frac{1}{\sqrt{\pi}}\sqrt{\frac{t}{\tau_{\rm Th}}(u(1-u))}+\frac{t}{\tau_{\rm Th}}(u(1-u))\,. \tag{1.40}$$

For larger n the exponential function in Eq. (1.38) can be expanded since the sum converges at $k\simeq 1$.

For $\tau_T\ll t$, $z(u)$ is large ($\sim -t/\tau_T$) in the interval $0<u<\tau_T/t$ and $z(u)\approx 1$ otherwise. Thus, it will be convenient to decompose $z(u)=\overline{z}+\tilde{z}(u)$ into a constant part $\overline{z}=+1$ and a peaked part $\tilde{z}(u)=z(u)-1$. For contributions of the peaked type one observes that

$$\int_0^1 {\rm d}u\,\tilde{z}(u)\,u^s=\begin{cases}-1, & s=0\,;\\ -\sqrt{\frac{\tau_T}{t}}\frac{\sqrt{2\pi}}{4}|\zeta\left(\frac{1}{2}\right)|, & s=1/2\,;\\ -\frac{\tau_T}{t}, & s=1\,.\end{cases} \tag{1.41}$$

We identify the following 3 regimes:

Diffusive regime $\tau_T\ll t\ll\tau_{\rm Th}$ and $n=0$: Here we can use the expansion Eq. (1.40). The constant term does not contribute, due to Eq. (1.39). The main contribution to the integral comes from values of u where $z(u)\approx 1$. Thus, we decompose $z(u)=\overline{z}+\tilde{z}(u)$ as suggested above. The leading result and corrections $\propto\sqrt{t/\tau_{\rm Th}}$ due to the second and third term in Eq. (1.40) stem from $\overline{z}$. Corrections $\propto\sqrt{t/\tau_T}$ can be calculated with the help of Eq. (1.41) with $s=1/2$ from the $\tilde{z}(u)$ part. In total we obtain for $n=0$:

$$\mathcal{F}_{n=0}(t)=\frac{\pi^{3/2}\sqrt{E_{\rm Th}}}{2g_1}\,Tt^{3/2}\left(1+\frac{2^{3/2}\zeta\left(\frac{1}{2}\right)}{\pi}\frac{1}{\sqrt{tT}}-\frac{4}{3\sqrt{\pi}}\sqrt{\frac{t}{\tau_{\rm Th}}}\right)\,. \tag{1.42}$$

Diffusive regime $\tau_T\ll t\ll\tau_{\rm Th}$ and $|n|>0$: For winding numbers larger than zero, we expand the exponential function in (1.38). In contrast to the case of $n=0$, the leading result comes here from the peaked part $\tilde{z}(u)$. After expanding the exponential function and doing the sum over k, we can apply Eq. (1.41) with $s=0$ and $s=1$ to find the leading result and a correction $\sim\tau_T/t$. For $\overline{z}$, we observe that the first term vanishes since the integral is over n full periods of cos. The second term of the expansion gives a correction $\sim t/\tau_{\rm Th}$ and in total for $0<|n|\ll t/\tau_T$:

$$\mathcal{F}_n(t)=\frac{\pi}{3g_1}\,Tt\left(1-\frac{2}{n^2}\frac{t}{\tau_{\rm Th}}-\frac{6}{\pi n}\frac{\tau_T}{t}\right)\,. \tag{1.43}$$

Note that in the diffusive regime, winding numbers $|n| > 0$ only contribute weakly to the conductivity, see Eq. (1.29).

Ergodic regime $\tau_T \ll \tau_{\rm Th} \ll t$: In this regime, the main contribution to the conductivity will not depend on n, since we may neglect the cos-term of $q_n(u)$ as long as $|n| \ll t/\tau_{\rm Th}$. This restriction on n is justified by the fact that large values of $|n|$ give contributions smaller by a factor of $\sim \exp(-n^2 t/\tau_{\rm Th})$, see Eq. (1.29).

Again, we decompose $z(u) = \overline{z} + \tilde{z}(u)$. For the $\tilde{z}(u)$ part, we use the expansion of $q_{n=0}(u)$, Eq. (1.40), where the constant term $1/12$ will yield the main result. Corrections due to the second term of Eq. (1.40) are $\sim \sqrt{\tau_T/\tau_{\rm Th}}$, because of Eq. (1.41) with $s = 1/2$. For $\overline{z}$, we do the integral over u directly using $\int_0^1 \mathrm{d}u\, \exp(-xu(1-u)) \xrightarrow{x\to\infty} 2/x$. From this we obtain a correction $\sim \tau_{\rm Th}/t$ and in total

$$\mathcal{F}_n(t) = \frac{\pi}{3g_1}\, Tt \left(1 - \frac{6}{\sqrt{2\pi}}\sqrt{\frac{\tau_T}{\tau_{\rm Th}}} - \frac{1}{30}\frac{\tau_{\rm Th}}{t}\right) . \tag{1.44}$$

It is not surprising that the case $|n| > 0$ in the diffusive regime gives, to leading order, the same results as all n of the ergodic regime (compare Eq. (1.44) to (1.43)), since higher winding numbers are by definition always ergodic: The electron paths explore the system completely.

$0D$ regime $\tau_{\rm Th} \ll \tau_T \ll t$: In this regime, $q_n(u)$ is more sharply peaked than $z(u)$, since $\tau_T/t \gg \tau_{\rm Th}/t$. This means that the electron reaches the fully ergodic limit (where $q(u) = \text{const}$ and no dephasing can occur) before the fluctuating potential changes significantly. Thus, the potential is effectively frozen and only small statistical deviations from the completely ergodic limit yield a phase difference between the two time-reversed trajectories. The width of the peak of $z(u)$ becomes unimportant, instead, we can expand $z(u)$ around $u = 0$ and $u = 1$. Furthermore, we can expand the argument of the exponential function in $q_n(u)$ and then extend the integral to $+\infty$ and scale u by $k\pi$:

$$\mathcal{F}_n(t) = \frac{4\pi Tt}{g_1}\int_0^\infty \mathrm{d}u \left[\frac{2\pi Tt}{3} - 1 - \frac{4\pi^3}{15}(tT)^3 u^2\right] \sum_{k=1}^{\infty} \frac{\cos(2nu)}{(k\pi)^3} e^{-4k\pi E_{\rm Th} tu} \tag{1.45}$$

(the -1 in the integrand stems from the region $u \approx 1$). Now, assuming $|n| \ll t/\tau_{\rm Th}$, the integral over u can be done and then the sum over k

evaluated. The result is

$$\mathcal{F}_n(t) = \frac{\pi^2 \tau_{\rm Th}}{270\, g_1}\, T^2 t \left(1 - \frac{3}{2\pi}\frac{1}{Tt} - \frac{\pi^2}{210}\frac{T^2}{E_{\rm Th}^2}\right) . \tag{1.46}$$

Note that, as mentioned before, the precise form of the shape of $\tilde{z}(u)$, corresponding to the broadened delta function Eq. (1.17), matters only in $0D$ regime.

To summarize, we found the following regimes:

$$\mathcal{F}_n(t) \simeq \begin{cases} \dfrac{\pi^{3/2}}{2g_1}\sqrt{E_{\rm Th}} T t^{3/2} & ,\tau_T \ll t \ll \tau_{\rm Th}, n = 0; \quad (1.47a) \\ \dfrac{\pi T t}{3 g_1}, & \tau_T \ll t \ll \tau_{\rm Th}, |n| > 0; \quad (1.47b) \\ \dfrac{\pi T t}{3 g_1}, & \tau_T \ll \tau_{\rm Th} \ll t, \text{all } n; \quad (1.47c) \\ \dfrac{\pi^2}{270\, g_1}\dfrac{T^2 t}{E_{\rm Th}}, & \tau_{\rm Th} \ll \tau_T \ll t, \text{all } n. \quad (1.47d) \end{cases}$$

Note that the crossover temperatures where $\tau_\varphi^{\rm diff} \simeq \tau_\varphi^{\rm erg}$ or $\tau_\varphi^{\rm erg} \simeq \tau_\varphi^{0D}$, namely $c_1 g_1 E_{\rm Th}$ or $c_2 E_{\rm Th}$, respectively, involve large prefactors, $c_1 = 27/4 \simeq 7$ and $c_2 = 90/\pi \simeq 30$. This can be seen in a numerical evaluation of Eq. (1.36), which is presented in Fig. 1.6. In particular, one observes that the onset of the $0D$ regime is already at temperatures smaller than $30 E_{\rm Th}$, i.e. well above $E_{\rm Th}$. This should significantly simplify experimental efforts to reach this regime.

1.7. Correction to the conductance

Inserting Eq. (1.29) into Eq. (1.4), we obtain the temperature dependent correction to the conductance

$$\Delta g(T,\phi) = -\frac{4L}{g_1 \tau_{\rm Th}} \int_0^\infty {\rm d}t \sum_{n=-\infty}^{+\infty} \frac{e^{-(n/2)^2 \tau_{\rm Th}/t}}{\sqrt{4\pi D t}} e^{-t/\tau_H - t/\tau_{\rm dw} - \mathcal{F}_n(t)} \cos(4\pi n\, \phi/\phi_0) . \tag{1.48}$$

The resulting value of $|\Delta g(T,\phi)|$ increases with decreasing T in a manner governed by τ_φ. We recall that in the high temperature regime dephasing

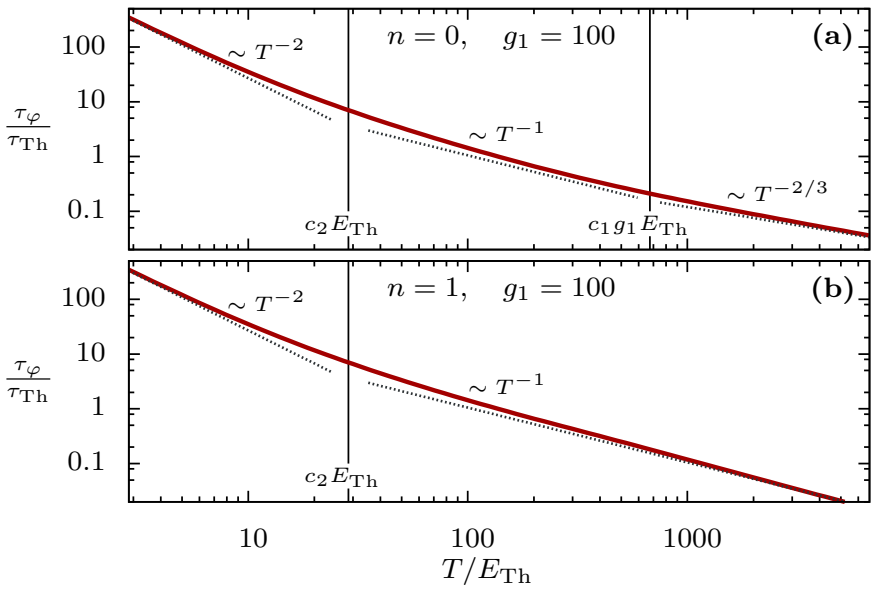

Fig. 1.5. Dephasing time τ_φ extracted from Eq. (1.36) and $\mathcal{F}_n(\tau_\varphi)=1$ for $g_1=100$. (a) Shows the result for zero winding number $n=0$ and (b) for $n=1$. For winding numbers $|n|>0$ the diffusive regime, $\tau_\varphi \sim T^{-2/3}$, is absent.

can be relatively strong, so that one can neglect effects of dissipation (i.e. particle escape out of the ring) and of the external magnetic field on the Cooperon if $\tau_\varphi(T) \ll \min[\tau_H, \tau_{\rm dw}]$. In the diffusive regime, $\tau_\varphi \ll \tau_{\rm Th}$, $\Delta g(T,\phi)$ is dominated by the trajectories with $n=0$ since the contribution of the trajectories with $|n| \geq 2\sqrt{t/\tau_{\rm Th}} \sim \sqrt{\tau_\varphi/\tau_{\rm Th}}$ is exponentially small. Thus we arrive at:[20]

$$|\Delta g| \simeq \frac{2}{g_1}\sqrt{\frac{\tau_\varphi}{\tau_{\rm Th}}} \propto \left(\frac{E_{\rm Th}}{g_1^2 T}\right)^{1/3} . \tag{1.49}$$

In contrast, the trajectories with large winding number contribute in the ergodic regime, $\tau_T \ll \tau_{\rm Th} \ll \tau_\varphi$, therefore, converting the sum to the integral $\sum_n \exp(-(n/2)^2\tau_{\rm Th}/t) \simeq \int {\rm d}n \exp(-(n/2)^2\tau_{\rm Th}/t) \sim \sqrt{t/\tau_{\rm Th}}$, Eq.(1.48) yields[24,25]

$$|\Delta g| \simeq \frac{4}{g_1}\frac{\tau_\varphi}{\tau_{\rm Th}} \propto \frac{E_{\rm Th}}{T} . \tag{1.50}$$

Dephasing due to electron interactions becomes *weak* in the $0D$ regime and, therefore, the situation drastically changes at the crossover from the

ergodic regime to the $0D$ one. In particular, we find $\tau_\varphi \gg g_1\tau_{\rm Th}$, see Eq.(1.47c) and as far as g_1 is large, one may enter a low temperature regime where $\tau_\varphi \geq \tau_{\rm dw}$. In this case, the temperature independent parts of the Cooperon decay must be taken into account. In our model, with decreasing T, the growth of $|\Delta g(T,\phi)|$ saturates towards $|\Delta g(0,\phi)|$ once τ_φ increases past $\min[\tau_H, \tau_{\rm dw}]$ (a more quantitative consideration is given in the next section). Nevertheless, the temperature dependence of Δg is still governed by $\tau_\varphi(T)$ and we can single it out by subtracting the conductance from its limiting value at $T = 0$. Then the difference

$$|\Delta g(0,\phi)| - |\Delta g(T,\phi)| \simeq \frac{4}{g_1}\frac{\tau_{\rm dw}^2}{\tau_{\rm Th}\tau_\varphi} \propto \left(\frac{\tau_{\rm dw}T}{g_1}\right)^2 \tag{1.51}$$

shows T^2-behaviour in the $0D$ regime.

1.8. Suggested Experiments

Our theoretical predictions should be observable in real experiments, provided that several requirements are met. We list these conditions in accordance with their physical causes, focusing below on the example of a ring prepared from a quasi-$1D$ wire of width L_W on a $2D$ surface.

1.8.1. *Validity of theoretical predictions*

$1D$ diffusion: We have used the theory of $1D$ diffusion which calls for the following inequalities

$$L \gg (\ell, L_W) \gg \lambda_{\rm F}\,; \tag{1.52}$$

$\lambda_{\rm F}$ is the Fermi wavelength.

Weak localization regime: Eq.(1.48) describes the leading weak localization correction to the conductance. Subleading corrections can be neglected if (a) the classical conductance of the ring is large

$$g_1 \propto (\ell/L)(L_W/\lambda_{\rm F}) \gg 1\,; \tag{1.53}$$

and (b) the leading correction to the conductivity is smaller than its classical value, $|\Delta g| < 1$. The former condition can be assured by a proper choice of the ring geometry and of the material while, in the low temperature regime, the latter is provided by finite dissipation.

Time-/spatial-dependence of the noise correlation function: We have used the noise correlation function (1.16) where dependences on time- and space-coordinates are factorized. This simplified form requires the following condition (see Section 1.3):

$$2\nu D\mathbf{q}^2 \gg (D\mathbf{q}^2 - i\omega)/V(\mathbf{q})\,. \tag{1.54}$$

In the $0D$ regime we can roughly estimate typical values, $D\mathbf{q}^2 \sim \omega \sim E_{\rm Th}$, arriving at the inequality

$$\nu V(\mathbf{q}) \gg 1\,. \tag{1.55}$$

For a quasi-$1D$ wire on a $2D$ structure, ν and V can be written as (restoring $\hbar$)

$$\nu_{\rm 2D} = \frac{m_e}{2\pi\hbar^2}\,, \tag{1.56}$$

where m_e is the electron mass, and

$$V_{\rm 1D}(q) = \frac{e^2 L_W}{4\pi\epsilon_0}|\ln(L_W^2 q^2)| \tag{1.57}$$

(in SI units). Thus, (1.55) implies that L_W cannot be taken to be overly small. Inserting material parameters, however, this condition turns out not to be very restrictive, as long as $\nu_{\rm 2D}$ is reasonably large.

Contacts (dissipation and absence of the Coulomb blockade): The presence of contacts, through which electrons can escape into leads, is mimicked in our model through the homogeneous dissipation rate $1/\tau_{\rm dw}$. We have assumed weak dissipation:

$$\tau_{\rm Th} \lesssim \tau_{\rm dw}\,. \tag{1.58}$$

This ensures that the winding trajectories with $|n| \geq 1$, responsible for AAS oscillations, are relevant. On the other hand, $\tau_{\rm dw}$ cannot be taken to be arbitrarily large, since the growth of the WL correction to the conductance with decreasing temperature is cut off mainly due to this temperature independent dissipation, and this cutoff has to occur sufficiently soon that the relative correction remains small, else we would leave the WL regime. Choosing the zero temperature limit, somewhat arbitrary, as $|\Delta g(0,\phi)| = 1/2$, we find from Eq. (1.50)

$$\tau_{\rm dw}/\tau_{\rm Th} \lesssim g_1/8\,. \tag{1.59}$$

We note that our assumptions imply $\tau_\varphi \gg g_1\tau_{\rm Th} > \tau_{\rm dw}$ in the $0D$ regime, i.e., dephasing due to electron interactions is weak (each electron contributing to transport through the ring is dephased only a little bit during the course of its stay in the ring). Nevertheless, we demonstrate below (see Fig. 1.8) that the T^2-dependence of the conductance should be visible in real experiments.

To choose a suitable value for the conductance at the contacts, we estimate $\tau_{\rm dw}/\tau_{\rm Th} \simeq g_1/g_{\rm cont}$, which results in

$$8 \lesssim g_{\rm cont}\,. \tag{1.60}$$

We suppose that the contacts are open and have a maximal transmission per channel at the contact

$$T_{\rm cont} = 1 \;\Rightarrow\; g_{\rm cont} = T_{\rm cont}N = N\,, \tag{1.61}$$

(N is the number of transmitting reflectionless channels at the contact). This choice allows one to maximize the WL effect and, simultaneously, to minimize any Coulomb blockade effects, which we have neglected.

1.8.2. *Possible experimental setup*

Temperature range: The relevant temperature range, $[T_{\rm dil}, T_{\rm ph}]$, is limited from below by dilution refrigeration ($T_{\rm dil} \simeq 10$mK) and from above by our neglect of phonons ($T_{\rm ph} \simeq 5$K). Furthermore, the ring should be small enough that $c_2E_{\rm Th} \gtrsim T_{\rm dil}$; $c_2E_{\rm Th}$ is the upper estimate for the temperature of the crossover to the $0D$ regime, see the discussion after Eq. (1.47).

Contributions from the leads: We have considered an ideal situation and calculated the Cooperon decay function for the isolated ring, where the finite dissipation rate $1/\tau_{\rm dw}$ does not affect the decay function up to leading order in $\tau_{\rm Th}/\tau_{\rm dw}$. This means that the Cooperons are assumed to live completely inside the ring and not influenced by dephasing in the leads, i.e. it corresponds to the situation shown in Fig. 1.6(a).

In real experiments, the correction to the conductance, Δg, is sensitive to dephasing in the leads because Cooperons exist which either belong to the lead (e.g. the situation shown in Fig. 1.6(c)) or extend over both the ring and the lead (Fig. 1.6(b))[49]. (Note that in contrast to Ref. [51] or Ref. [49], we do not consider Cooperons with a Hikami-box directly at the contact, since we chose $T_{\rm cont} = 1$.)

Contributions of such trajectories might mask the signatures of dephasing in the confined region (the ring). This concern also applies to

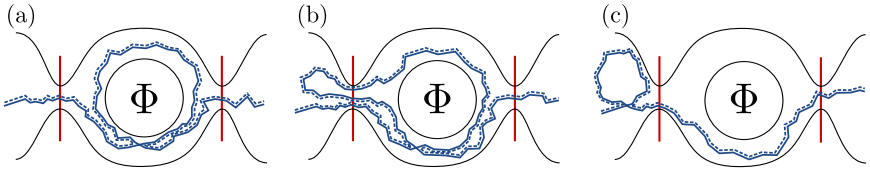

Fig. 1.6. (a) a "ring"-Cooperon, confined entirely to the ring; (b) a "cross"-Cooperon, extending from the ring to the lead and back; (c) a "lead"-Cooperon, confined entirely to the leads.

quantum dots connected to leads (cf. the $\tau_\varphi \propto T^{-1}$-behavior observed in Refs. [31–33]), or finite-size effects in a network of disordered wires,[35] where paths encircling a given unit cell might spend significant time in neighboring unit cells as well (cf. $T^{-1/3}$-behavior observed in Ref. [35] at $\tau_\varphi/\tau_{\rm Th} \geq 1$).

We will now argue that if the lead dimensionless conductance is larger than the contact conductance[50]

$$g_{\rm lead} \gg g_{\rm cont} = N\,, \tag{1.62}$$

then the ring-Cooperon yields the dominating contribution to the WL corrections. Let us focus on the ergodic and 0D regimes, for which $\tau_\varphi \gg \tau_{\rm Th}$, so that that the Cooperon ergodically explores the entire ring. Then the probability to find a closed loop in the ring is proportional to the dwell time, $p_{\rm ring} \propto \tau_{\rm dw}/\nu$, which is $\propto 1/g_{\rm cont}$. Thus we can estimate:

- the probability to enter the ring as $p_{\rm in} \sim g_{\rm cont}/g_{\rm lead}$;
- the probability to find a closed loop in the ring as $p_{\rm ring} \sim (\tau_{\rm dw}/\nu) \sim 1/g_{\rm cont}$;
- the probability to exit the ring as $p_{\rm out} \sim (\tau_{\rm dw}/\nu) g_{\rm cont} \sim 1$;
- the probability to find a closed loop in the diffusive lead as $p_{\rm lead} \sim 1/g_{\rm lead}$

Using these estimates, the probabilities to find a ring-, cross-, or lead-Cooperon are

$$P_{\rm C-ring} \sim p_{\rm in} \times p_{\rm ring} \times p_{\rm out} \sim 1/g_{\rm lead}\,; \tag{1.63}$$

$$P_{\rm C-cross} \sim p_{\rm in} \times p_{\rm ring} \times p_{\rm out} \times p_{\rm in} \times p_{\rm out} \sim g_{\rm cont}/g_{\rm lead}^2\,; \tag{1.64}$$

$$P_{\rm C-lead} \sim p_{\rm lead} \times p_{\rm in} \times p_{\rm out} \sim g_{\rm cont}/g_{\rm lead}^2\,, \tag{1.65}$$

respectively. Thus we arrive at:

$$P_{\rm C-lead} \sim P_{\rm C-cont} \sim P_{\rm C-ring} \times g_{\rm cont}/g_{\rm lead} \ll P_{\rm C-ring}\,, \tag{1.66}$$

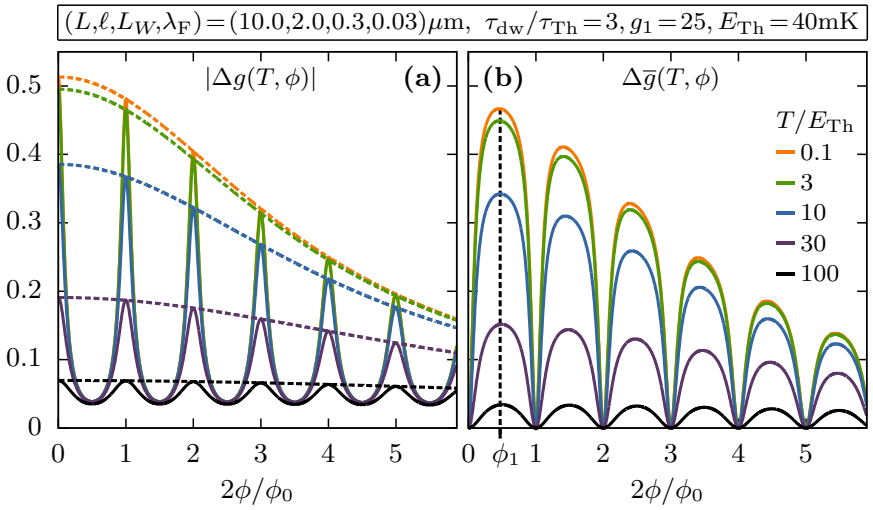

Fig. 1.7. (a) The WL correction $|\Delta g(T,\phi)|$ (solid lines), its envelope $|\Delta g_{\rm en}(T,\phi)|$ (dashed lines) and (b) their difference $\Delta\bar{g} = |\Delta g_{\rm en}| - |\Delta g|$, plotted as function of magnetic flux $2\phi/\phi_0$, for five different temperatures.

which proves that the ring-Cooperon dominates the WL correction for our choice of parameters if $g_{\rm lead} \gg g_{\rm cont}$.

Since the $0D$ regime implies weak dephasing it is highly desirable to improve the "signal-to-noise" ratio by filtering out contributions which do not show $0D$ dephasing. This can be done[35] by constructing from $|\Delta g(T,\phi)|$ its nonoscillatory envelope $|\Delta g_{\rm en}(T,\phi)|$, obtained by setting $\theta = 0$ in Eq. (1.29) while retaining $\tau_H \neq 0$, and studying the difference

$$\Delta\bar{g}(T,\phi) = |\Delta g_{\rm en}(T,\phi)| - |\Delta g(T,\phi)|\,. \tag{1.67}$$

This procedure is illustrated in Fig. 1.7. The lead-Cooperons do not have the Aharonov-Bohm phase and are eliminated by this filtering procedure. Unfortunately, cross-Cooperons cannot be filtered in this manner, since they do experience the Aharonov-Bohm phase. Nevertheless, if the condition $g_{\rm cont} \ll g_{\rm lead}$ holds, $\Delta\bar{g}$ is completely dominated by paths residing only in the ring in accordance with the estimate Eq. (1.66).

1.8.3. *Numerical results for 2D GaAs/AlGaAs heterostructures*

All above-mentioned constraints can be met, e.g., with rings prepared from a $2D$ GaAs/AlGaAs heterostructure. In such systems, diffusive behavior

emerges from specular boundary scattering of the electrons, see Ref. [46], leading to the following dephasing time due to the external magnetic field:

$$\tau_H = 9.5(c/eH)^2 \times (l/DL_W^3)\,. \tag{1.68}$$

Furthermore, inserting Eq. (1.56) into the $2D$ conductivity $\sigma_{2\mathrm{D}} = 2e^2\nu_{2\mathrm{D}}D$ with $D = v_{\mathrm{F}}\ell$, we obtain the corresponding dimensionless conductance:

$$g_1 = \frac{h}{e^2}\frac{\sigma_{2\mathrm{D}}L_W}{L} = 4\pi\frac{L_W\ell}{\lambda_F L}\,. \tag{1.69}$$

A typical Fermi wavelength in a GaAs/AlGaAs heterostructure is $\lambda_{\mathrm{F}} \approx$ 30nm ($v_F \approx 2.5\cdot 10^5$m/s).[28,35,39,47] Thus, by suitably choosing L, L_W and ℓ we can adjust g_1 and E_{Th} to make all regimes of the dephasing time accessible.

Numerical results for $|\Delta g|$ and $\Delta\overline{g}$, obtained from Eq.(1.4) using experimentally realizable parameters, are shown in Figs. 1.7 and 1.8 for several combinations of these parameters. The regime where Δg exhibits diffusive $T^{-1/3}$ behavior ($7g_1E_{\mathrm{Th}} \ll T \ll T_{\mathrm{ph}}$) is visible only for our smallest choices of both g_1 and E_{Th} (Fig. 1.8(a), heavy dashed line). AAS oscillations in $|\Delta g|$ and $\Delta\overline{g}$ (Fig. 1.7), which require $\tau_{\mathrm{Th}} \ll \tau_\varphi$, first emerge at the crossover from the diffusive to the ergodic regime. They increase in magnitude with decreasing T, showing ergodic T^{-1} behavior for $30E_{\mathrm{Th}} \ll T \ll 7g_1E_{\mathrm{Th}}$ (Figs. 1.8(a),(b)), and eventually saturate towards their $T = 0$ values, with $\Delta\overline{g}(0,\phi) - \Delta\overline{g}(T,\phi)$ showing the predicted $0D$ behavior, $\propto T^2$, for $T \lesssim 5E_{\mathrm{Th}}$, see Fig. 1.8(c).

1.9. Conclusions

For an almost isolated disordered quasi-$1D$ ring with $T \gg E_{\mathrm{Th}}$, the T-dependence of the dephasing time has been known to behave as $\tau_\varphi \propto T^{-2/3}$ (Ref. [20]) or $\propto T^{-1}$ (Refs. [24,25]) in the diffusive or ergodic regimes, respectively. Here we showed how it crosses over, for $T \ll 30E_{\mathrm{Th}}$, to $\tau_\varphi \propto T^{-2}$, in agreement with the theory of dephasing in $0D$ systems (Ref. [2]). This crossover manifests itself in both the smooth part of the magnetoconductivity and the amplitude of the AAS oscillations. Importantly, the latter fact can be exploited to decrease the effects of dephasing in the leads, by subtracting from the magnetoconductivity its smooth envelope. While we did not give an exhaustive study of all contributions to dephasing in the connected ring, we were able to show that the leading contribution results only from trajectories confined to the ring. Thus, an analysis of the T-dependence of the AAS oscillation amplitude may offer

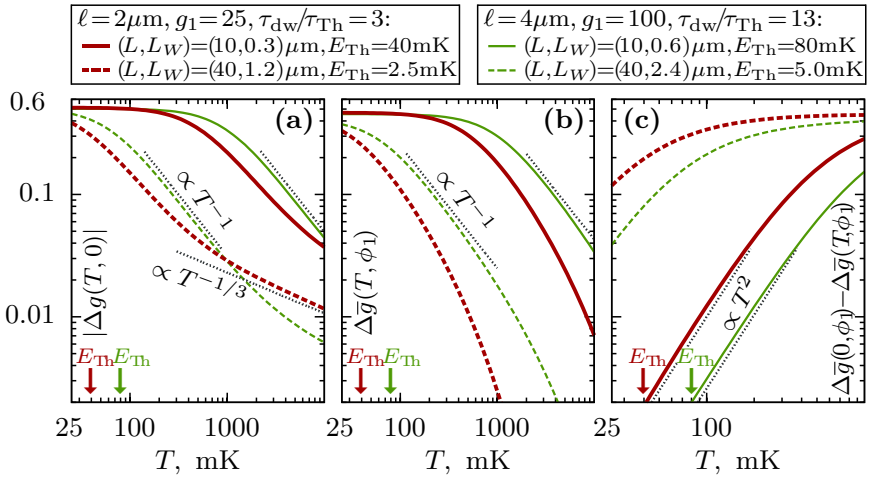

Fig. 1.8. T-dependence of (a) the WL correction at zero field, $|\Delta g(T,0)|$ and (b) at finite field with envelope subtracted, $\Delta\bar{g}(T,\phi_1)$; (c) the difference $\Delta\bar{g}(0,\phi_1)-\Delta\bar{g}(T,\phi_1)$, which reveals a crossover to T^2-behavior for $T \ll 30E_{\rm Th}$. The flux ϕ_1, which weakly depends on T, marks the first maximum of $\Delta\bar{g}(T,\phi)$, see inset of Fig. 1.7. [This figure is reproduced from Ref. [1]]

a way to finally observe, for $T \lesssim 5E_{\rm Th}$, the elusive but fundamental $0D$ behavior $\tau_\varphi \sim T^{-2}$. Its observation, moreover, would allow *quantitative* experimental tests of the role of temperature as ultraviolet frequency cut-off in the theory of dephasing. An interesting challenge for future works consists in a more realistic model of the connection to the leads. Work on the model of an N-channel ring attached via two arms with fewer channels to absorbing boundaries is currently in progress.[52]

Acknowledgments

We acknowledge illuminating discussions with B. L. Altshuler, C. Bäuerle, N. O. Birge, Ya. M. Blanter, P. W. Brouwer, L. I. Glazman, Y. Imry, V. E. Kravtsov, J. Kupferschmidt, A. D. Mirlin, Y. V. Nazarov, A. Rosch, D. Weiss and V. I. Yudson. We acknowledge support from the DFG through SFB TR-12, the Emmy-Noether program and the Nanosystems Initiative Munich Cluster of Excellence; from the NSF, Grant No. PHY05-51164; and from the EPSRC, Grant No. T23725/01.

References

1. M. Treiber, O. M. Yevtushenko, F. Marquardt, J. von Delft, and I. V. Lerner, Phys. Rev. B **80**, 201305(R) (2009).
2. U. Sivan, Y. Imry, and A. G. Aronov, Europhys. Lett. **28**, 115 (1994).
3. Y. Imry, in *Introduction to Mesoscopic Physics*, Oxford University Press (1997)
4. M. Büttiker, Y. Imry, and R. Landauer, Phys. Rev. A **96**, 365 (1983).
5. M. Büttiker, Y. Imry, and M. Ya. Azbel, Phys. Rev. A **30**, 1982 (1984).
6. Y. Gefen, Y. Imry, and M. Ya. Azbel, Phys. Rev. Lett. **52**, 129 (1984).
7. M. Büttiker, Y. Imry, R. Landauer, and S. Pinhas, Phys. Rev. B **31**, 6207 (1984).
8. M. Murat, Y. Gefen, and Y. Imry, Phys. Rev. B **34**, 659 (1985).
9. Y. Imry, and N. S. Shiren, Phys. Rev. B **33**, 7992 (1986).
10. A. D. Stone, and Y. Imry, Phys. Ref. Lett. **56**, 189 (1986).
11. B. L. Altshuler, Y. Gefen, and Y. Imry, Phys. Rev. Lett. **66**, 88 (1990).
12. L. P. Levy, G. Dolan, J. Dunsmuir, and H. Bouchiat, Phys. Rev. Lett. **64**, 2074 (1990).
13. H. Bluhm, N. C. Koshnick, J. A. Bert, M. E. Huber, and K. A. Moler, Phys. Rev. Lett. **102**, 136802 (2009).
14. A. C. Bleszynski-Jayich, W. E. Shanks, B. Peaudecerf, E. Ginossar, F. von Oppen, L. I. Glazman, and J. G. E. Harris, arXiv:0906.4780 (2009).
15. Y. Imry, Physics **2**, 24 (2009).
16. R. A. Webb, S. Washburn, C. P. Umbach, and R. B. Laibowitz, Phys. Rev. Lett. **54**, 2696 (1985).
17. B. L. Altshuler, A. G. Aronov, and B. Z. Spivak, JETP Lett. **33**, 94 (1981).

18. D. Y. Sharvin, and Y. V. Sharvin, Pis'ma Zh. Teor. Eksp. Fiz. **34**, 285 (1981).
19. A. Stern, Y. Aharonov, and Y. Imry, Phys. Rev. A **41**, 3436 (1990).
20. B. L. Altshuler, A. G. Aronov, and D. E. Khmelnitsky, J. Phys. C **15**, 7367 (1982).
21. H. Fukuyama and E. Abrahams, Phys. Rev. B, **27**, 5976 (1983).
22. B. L. Altshuler and A. G. Aronov, in *Electron-Electron Interactions in Disordered Systems*, edited by A. L. Efros and M. Pollak, North-Holland, Amsterdam, 1 (1985).
23. I. L. Aleiner, , B. L. Altshuler, and M. E. Gershenson, Waves in Random Media **9**, 201 (1999).
24. T. Ludwig and A. D. Mirlin, Phys. Rev. B **69**, 193306 (2004).
25. C. Texier and G. Montambaux, Phys. Rev. B **72**, 115327 (2005).
26. F. Marquardt, J. von Delft, R. A. Smith, and V. Ambegaokar, Phys. Rev. B **76**, 195331 (2007).
27. J. von Delft, F. Marquardt, R. A. Smith, and V. Ambegaokar, Phys. Rev. B **76**, 195332 (2007).
28. C. M. Marcus, R. M. Westervelt, P. F. Hopkins, and A. C. Gossard, Phys. Rev. B **48**, 2460 (1993).
29. A. Yacoby, M. Heiblum, H. Shtrikman, V. Umansky, and D. Mahalu, Semicond. Sci. Tech. **9**, 907 (1994).
30. B. Reulet, H. Bouchiat, and D. Mailly, Europhys. Lett. **31**, 305 (1995).
31. A. G. Huibers, M. Switkes, C. M. Marcus, K. Campman, and A. C. Gossard, Phys. Rev. Lett. **81**, 200 (1998);
32. A. G. Huibers, S. R. Patel, C. M. Marcus, P. W. Brouwer, C. I. Duruz, and J. S. Harris, Jr., Phys. Rev. Lett. **81**, 1917 (1998);
33. A. G. Huibers, J. A. Folk, S. R. Patel, C. M. Marcus, C. I. Duruz and J. S. Harris, Jr., Phys. Rev. Lett. **83**, 5090 (1999).
34. A. B. Gougam, F. Pierre, H. Pothier, D. Esteve, and N. O. Birge, J. Low Temp. Phys. **118**, 447 (2000).
35. M. Ferrier, A. C. H. Rowe, S. Gueron, H. Bouchiat, C. Texier, and G. Montambaux, Phys. Rev. Lett. **100**, 146802 (2008).
36. I. L. Aleiner, B. L. Altshuler, and Y. M. Galperin, Phys. Rev. B **63**, 201401 (2001).
37. I. L. Aleiner and Y. M. Blanter, Phys. Rev. B **65**, 115317 (2002).
38. Y. Imry, arXiv: cond-mat/0202044 (2002)
39. Y. Niimi, Y. Baines, T. Capron, D. Mailly, F.-Y. Lo, A. D. Wieck, T. Meunier, L. Saminadayar, and C. Bäuerle, Phys. Rev. Lett. **102**, 226801 (2009).
40. L. P. Gor'kov, A. I. Larkin, and D. E. Khmel'nitskii, JETP Lett. **30**, 228 (1979).
41. E. Akkermans and G. Montambaux, *Mesoscopic physics of electrons and photons* (Cambridge University Press, Cambridge, 2007).
42. D. E. Khmelnitskii, Physica B&C **126**, 235 (1984).
43. B. L. Altshuler and A. G. Aronov, JETP Lett. **33**, 499 (1981).
44. P. W. Brouwer and C. W. J. Beenakker, Phys. Rev. B **55**, 4695 (1997);
45. E. McCann and I. V. Lerner, Phys. Rev. B **57**, 7219 (1998).
46. C. W. J. Beenakker and H. van Houten, Phys. Rev. B **38**, 3232 (1988).

47. O. Yevtushenko, G. Lütjering, D. Weiss, and K. Richter, Phys. Rev. Lett. **84**, 542 (2000).
48. B. L. Altshuler, A. G. Aronov, and P. A. Lee, Phys. Rev. Lett. **44**, 1288 (1980).
49. Ya. M. Blanter, V. M. Vinokur, and L. I. Glazman, Phys. Rev. B **73**, 165322 (2006).
50. J. N. Kupferschmidt, and P. W. Brouwer, (private communication).
51. R. S. Whitney, Phys. Rev. B **75**, 235404 (2007).
52. M. Treiber, O. M. Yevtushenko, F. Marquardt, J. von Delft, and I. V. Lerner, to be published.